J. CHEM. SOC. FARADAY TRANS., 1991, 87(6), 815–823

Kinetics of Pyrolysis of Furan

Phillip P. Organ and John C. Mackie*
Department of Physical Chemistry, University of Sydney, NSW 2006, Australia

The kinetics of pyrolysis of furan vapour diluted in argon have been studied behind reflected shock waves in a shock tube both by time-resolved infrared CO_2 laser absorption spectrometry and by single pulse shock techniques of product analysis over the temperature range 1100–1700 K, at pressures of *ca.* 20 atm and at uniform residence times of *ca.* 300 μs. The rate of overall disappearance of furan, as measured by absorption spectrometry, was found to be first order in furan concentration, with a rate constant of $k_{overall} = 10^{15.3\pm0.3}$ exp[−326(±8) kJ mol^{-1}/RT] s^{-1} in agreement with a previous determination by Lifshitz *et al.* (A. Lifshitz, M. Bidani and S. Bidani, *J. Phys. Chem.*, 1986, **90**, 5373). Principal products were carbon monoxide, C_3H_4 (propyne and allene) and acetylene. Ketene was identified in the products by FTIR spectroscopy.

A detailed chemical reaction model for the pyrolysis was developed and shown to give good predictions of the concentration profiles of furan and the major products. Modelling and thermochemical considerations led to the postulate that the initiation of pyrolysis takes place by C—O bond scission to a biradical which can undergo decomposition, *via* parallel reaction paths, to the observed products.

Furan and its derivatives are important intermediates in the burning of low-rank coals and have been identified as air pollutants from fuel conversion facilities[1] and as major components in tobacco smoke.[2] Furans are also derived from biomass decomposition and conversion of biomass to fuels and high-valued chemicals is an increasingly important alternative to the non-renewable resources. The furan ring is an important structural grouping in low-rank coals[3] and the low-temperature thermal decomposition of coals is expected to lead to slow but irreversible modification of furan rings. A knowledge of the kinetics of pyrolysis of furan can help elucidate this modification and assist in the understanding of processes leading to increased coal reactivity upon thermal treatment[3] and the production of oxides of carbon from coal and biomass.

There are only two previous investigations of the kinetics of the thermal decomposition of furan. Grela *et al.*[4] studied the very low pressure pyrolysis (VLPP) of furan over the temperature range 1050–1270 K. Only the major products carbon monoxide and C_3H_4 (allene/propyne) were observed by mass spectrometry. They considered that the pyrolysis of furan took place by a simple unimolecular elimination of CO and from an extrapolation of their VLPP rate data arrived at a value of $k_\infty = 10^{15.6}$ exp(−308 kJ mol^{-1}/RT) s^{-1} for disappearance of furan.

Lifshitz *et al.*[5] studied the pyrolysis kinetics of furan diluted in argon in a single-pulse shock tube (SPST) between 1050 and 1460 K and at pressures of *ca.* 3 atm.† From detailed product analyses they considered that decomposition of furan took place by two parallel reaction channels, one producing CO and propyne, the second channel producing acetylene and ketene. Lifshitz *et al.*[5] obtained the value of $k_{overall} = 10^{15.43\pm0.45}$ exp[(−328 ± 8) kJ mol^{-1}/RT] s^{-1} for the overall disappearance of furan, about a factor of 10 lower than that of Grela *et al.*[4] at 1200 K. Although they measured several products, Lifshitz *et al.*[5] were unable to detect ketene in their reaction mixtures.

In view of the two discrepant values for the rate constant for disappearance of furan and because of the inability of previous researchers to observe ketene, the expected product of a postulated reaction channel, it would appear that a third study of the kinetics of pyrolysis of furan is warranted. Our present study, also carried out in part by SPST, not only provides an additional value of the rate constant for disappearance of furan but also develops and evaluates a detailed chemical kinetic reaction model for furan pyrolysis. In addition, we report a direct kinetic measurement of the decomposition of furan in highly dilute mixtures of argon by time-resolved IR spectroscopy.

† 1 atm = 101 325 Pa.

Experimental

Three mixtures of furan in argon (0.2, 1.0 and 2.0 mol.%) were pyrolysed behind reflected shocks in a shock tube of 76 mm i.d. The shock tube and ancillary gas analysis system when operating in the SPST mode have been described previously.[6] Temperatures ranged from 1100 to 1700 K and pressures behind the reflected shock front were *ca.* 15–22 atm. The uniform residence time behind the reflected shock wave was *ca.* 300 μs determined from pressure–time profiles recorded by Kistler gauges. Both incident and reflected shock velocities were measured and pressures and temperatures behind the reflected shock wave were computed from both measured velocities.

For IR studies the shock tube was equipped with pairs of germanium windows through which was directed the beam of a tunable waveguide CO_2 laser, constructed after the design of Gerlach and Amer.[7] The IR spectrum of furan vapour in argon behind the reflected shock was measured at a distance of 35 mm from the endwall using the CO_2 laser line 10P(14) (10.54 μm). This line has a coincidence with the furan absorption spectrum at high temperatures. The time constant of the optical system, mercury cadmium telluride detector, oscilloscope and ancillary circuitry was ⩽5 μs.

Furan samples were from Merck (stated purity 98%). Several bulb-to-bulb distillations were used to produce samples of purity >99.9% (by GC). Products methane, ethane, ethylene, acetylene, propene, propyne, allene, 1,3-butadiene, vinylacetylene, diacetylene and benzene, together with unreacted furan, were analysed by GC using a flame ionization detector (FID) on alumina and Porapak Q packed columns and a methyl siloxane 0.53 mm i.d. capillary column (SGE BP1). Carbon monoxide was separated on a Carbosphere column, converted to methane by means of a ruthenium methanizer and detected by FID. Hydrogen was analysed by a thermal conductivity detector. Product identification of the above was made by direct comparison with standards, matching retention times on all three columns. With the exception of vinylacetylene and diacetylene, commercial standards were available. Vinylacetylene was synthesized[8] by refluxing a mixture of 1,4-dichlorobut-2-ene

and KOH. Diacetylene was synthesized from 1,4-dichlorobut-2-yne according to the method of Armitage *et al.*[9]

Product mixtures were also analysed by Fourier-transform infrared spectroscopy (FTIR). Products positively identified from their FTIR spectra were allene, propyne, vinylacetylene, methane, carbon monoxide, benzene and ketene. Ketene concentrations were determined by measuring the FTIR spectra of the product mixture at a spectral resolution of 0.25 cm^{-1}, subtracting the overlapping CO peaks and calculating the concentration from previous measurements of the molar absorption coefficients.[10] Ketene in the product mixture was found to be very labile. It was necessary to determine its concentration immediately upon firing the shock. Because the ketene concentration in the product gas progressively decreased with time after the run, it was necessary to measure the ketene spectrum in the product mixture as a function of time. An extrapolation of the measured ketene concentrations back to the time of running the shock was then possible. This extrapolation procedure limited the precision in measurement of ketene concentrations to $\pm 20\%$. A GC peak associated with ketene was also observed in chromatograms of products using the methyl siloxane capillary column. The concentration obtained by FTIR agreed well with that obtained by GC (assuming a relative FID response for ketene equal to that of methane).

Mass balances of products and unreacted furan based on oxygen were always within $\pm 5\%$. Above 1600 K a progressive loss of carbon was observed and some soot formation was evident, on the walls of the shock tube after venting, in runs above 1600 K.

Results

Product Distributions

At the lowest temperatures at which decomposition of furan could be detected (*ca.* 1200 K) carbon monoxide, C_3H_4 (allene and propyne) and acetylene were observed in the products. Carbon monoxide was always the major product of pyrolysis. At the lowest temperatures, C_3H_4 (allene and propyne) were the major hydrocarbon products. At *ca.* 1500 K, yields of C_3H_4 passed through a maximum at *ca.* 40% yield. Above this temperature an acceleration in the rate of increase in yield of acetylene with temperature was observed. Yields of H_2 became significant only above 1500 K at which temperature the extent of furan conversion was 85%. Minor hydrocarbon products observed were methane, ethene, benzene, vinylacetylene and buta-1,3-diene. Temperature dependences of the furan remaining and of the products' yields are shown in Fig. 1–7. In these figures the indicated temperature is the gas temperature immediately behind the reflected shock front.

There is little difference in the normalized product distributions between the three mixture compositions studied. With the exception of ketene and hydrogen, the yield of products were in satisfactory agreement both qualitatively and quantitatively with those reported by Lifshitz *et al.*[5] who did not detect ketene nor analyse for H_2. The identification of ketene in the products is definitive as shown in Fig. 8 in which the product FTIR spectrum and difference spectrum of ketene around 2150 cm^{-1} are shown.

The ratio of $[C_2H_2]:[CH_2CO]$ was always greater than unity with only small amounts of ketene (<3 product mol%) being recorded. Yields of methane, ethene, vinylacetylene and benzene became appreciable only at temperatures above 1400 K.

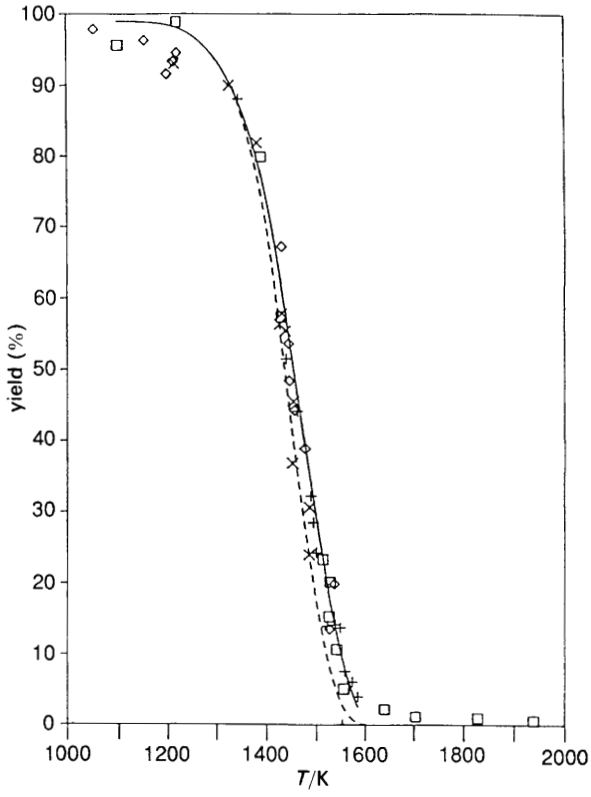

Fig. 1 Fraction of furan remaining in furan pyrolysis as a function of reflected shocked gas temperature. □, 1.0%; +, 2.0%; ◇, 0.2%; ×, 2.0%; (– –), model 2.0%; (——), model 0.2%; (Fig. 1–7)

Time-resolved Kinetic Measurements

An oscilloscope trace of the 10.54 μm absorption by a shock-heated furan mixture (2.0 mol.%) is shown as a function of time in Fig. 9. Also shown is the pressure profile measured at

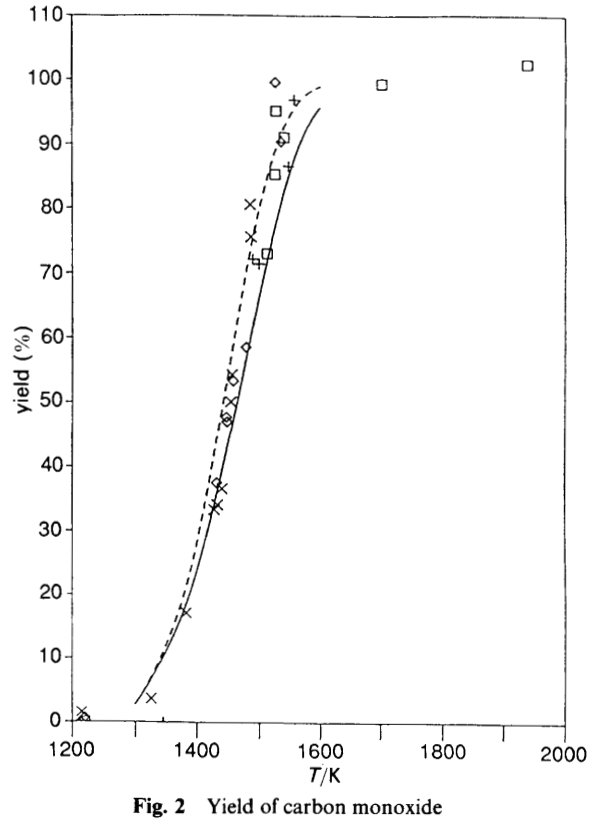

Fig. 2 Yield of carbon monoxide

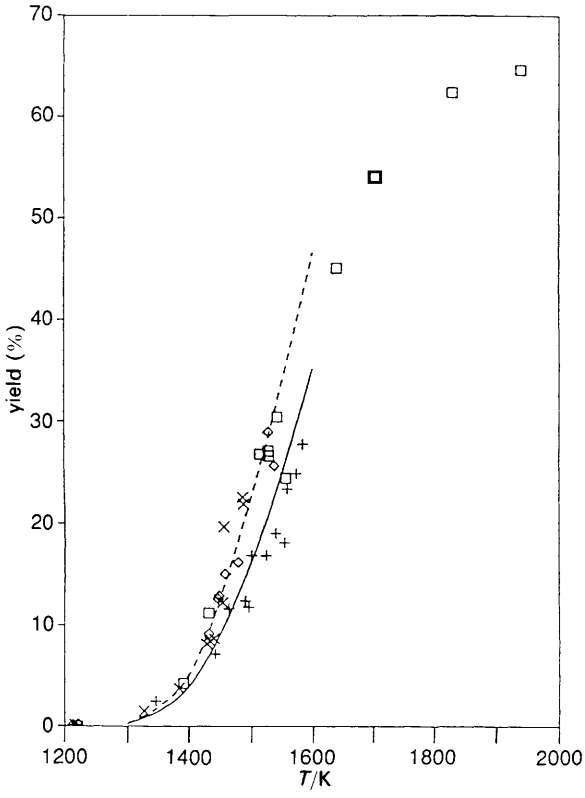

Fig. 3 Yield of acetylene

the same distance from the endwall. Two schlieren spikes are evident in the absorption spectrum, corresponding to the arrival, respectively, of the incident and reflected shock fronts at the observation window. The absorption coefficient for 10.54 μm radiation at room temperature is very low.

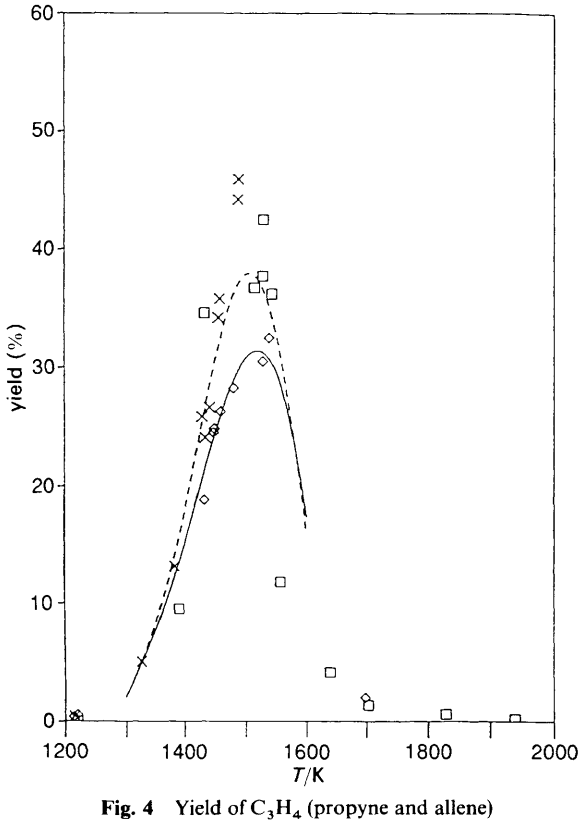

Fig. 4 Yield of C_3H_4 (propyne and allene)

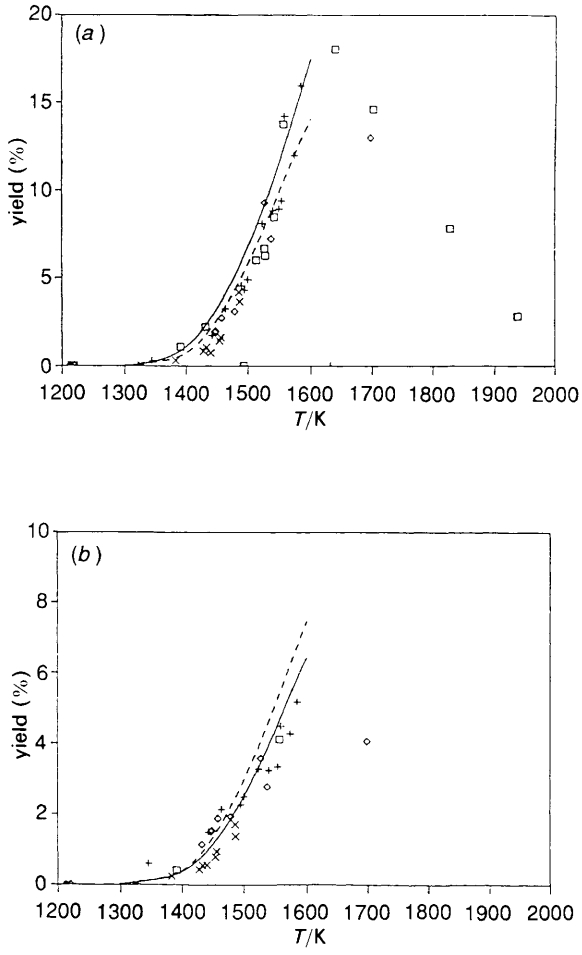

Fig. 5 (*a*) Yield of methane; (*b*) yield of ethylene as a function of reflected shocked gas temperature

However, the increased absorption coefficient at the temperature of the incident shocked gas leads to the observed absorption immediately following the incident shock front. Following the second schlieren spike is the exponential decay of the furan absorption resulting from thermal decomposition.

Because of poor signal-to-noise ratio, it was not possible to carry out kinetic analyses on furan absorption profiles for mixtures of furan <2.0 mol.%. In the 2.0% mixtures in argon, pyrolysis of furan is sufficiently endothermic to lead to significant temperature decreases in the adiabatic system. For $>99\%$ decomposition of the initial furan, the temperature drop in the 2.0% mixtures was *ca.* 140 K. Thus, the decaying profiles of Fig. 9 are not isothermal and part of the decrease in absorption results from a decrease in density. This effect must be accounted for in kinetic analysis of the absorption profiles. The following procedure was therefore used to analyse the IR absorption profiles.

The usual shock tube terminology[11] was adopted and conditions in the shocked gas behind the reflected shock wave were denoted by subscript 5. Because furan does not have any appreciable absorption at 10.54 μm at room temperature, the absorption coefficient, β_5, can be determined directly from the intensity, I_5, immediately after passage of the reflected shock front and the known initial concentration of furan immediately behind the shock front, C_5, the initial intensity, I_0, and the pathlength, l, by

$$\log(I_5/I_0) = -\beta_5 C_5 l \qquad (1)$$

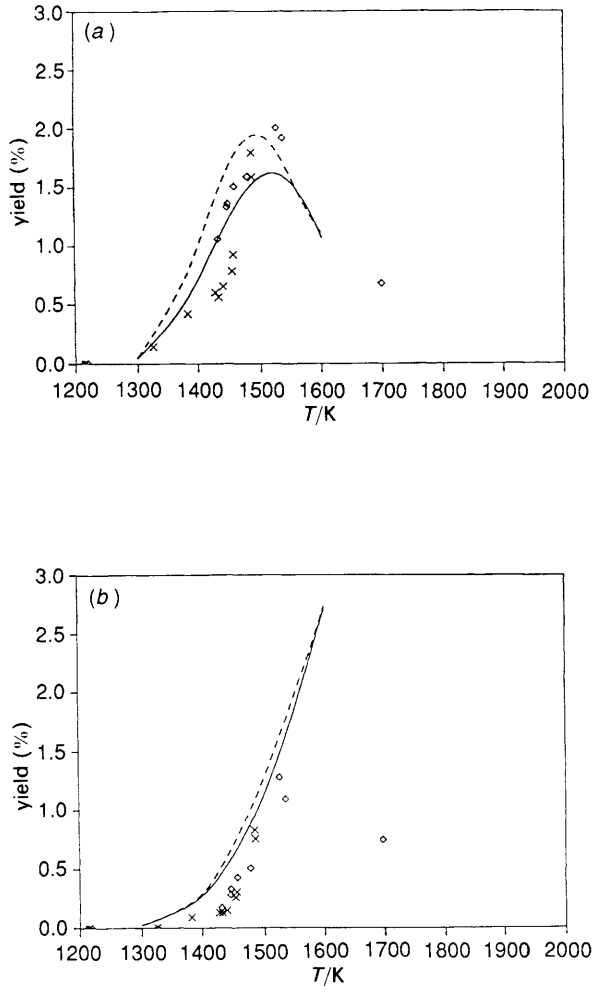

Fig. 6 (*a*) Yield of buta-1,3-diene; (*b*) yield of vinylacetylene

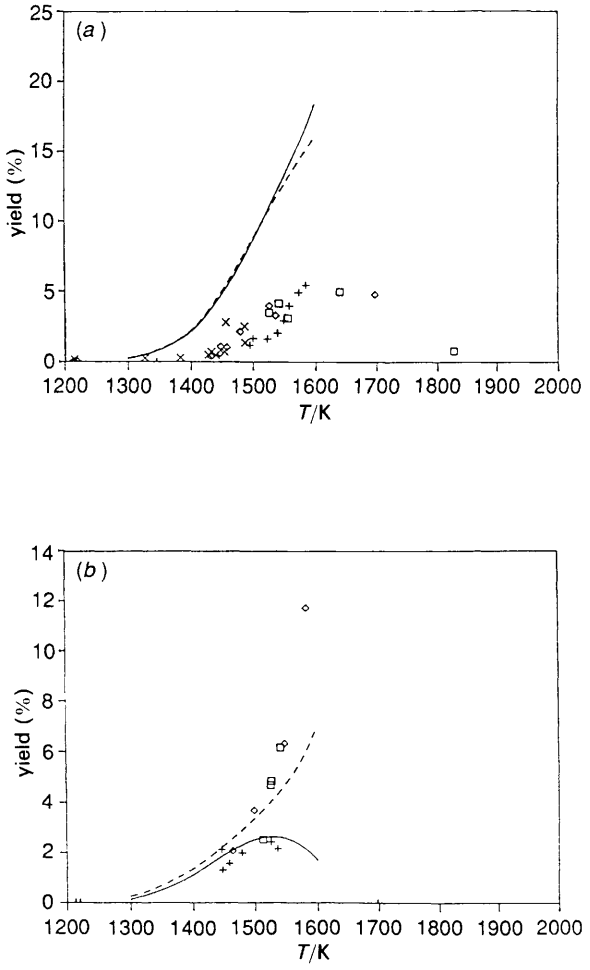

Fig. 7 (*a*) Yield of benzene; (*b*) yield of ketene and hydrogen. +, ketene data points; (——) model

Once β_5 is known, the concentration of furan, C_t, at time t, can be determined from values of I_t and I_0. The decrease in temperature due to reaction cooling is obtained as follows. If ΔH_r is the enthalpy of reaction, c_p is the molar heat capacity of the gas mixture and C_{tot} is the total concentration of the gas, then

$$-dC_t/dt = -(C_{tot}\, c_p/\Delta H_r)\, dT/dt \qquad \text{(ii)}$$

Since c_p is essentially constant with temperature (the gas is 98% Ar) and ΔH_r varies only slightly over the temperature range of the absorption profiles, eqn. (ii) may be rearranged to

$$dT/dC_t = (\Delta H_r/C_{tot}\, c_p) = B = \text{constant} \qquad \text{(iii)}$$

Integration of eqn. (iii) gives

$$T_5 - T = B(C_5 - C_t) \qquad \text{(iv)}$$

Substitution into the Arrhenius form of the first-order rate constant leads to

$$-dC_t/dt = A \exp[-E_a/R(T_5 - BC_5 + BC_t)] \qquad \text{(v)}$$

where A and E_a are the Arrhenius parameters.

It was assumed that the initial decay of furan was first order in the reactant. The first-order assumption was later verified in the SPST studies which showed an invariance of the rate of decay of furan upon initial concentration in mixtures of 2.0 and 0.2% furan in argon (see below.) A least-squares iterative routine together with an ordinary differential equation solver was then used to fit eqn. (v) to the experimental intensity profiles. A typical fitted profile is shown in Fig. 9. Because the decrease in temperature through the absorption profile is not large, the fit was not very sensitive to the individual values of A and E_a. It was, however, very sensitive to the absolute value of the rate constant $k = A \exp(-E_a/RT)$ and fitted values for the rate constant for each run could be determined with an uncertainty of $< \pm 10\%$.

An Arrhenius plot of the first-order rate constants for disappearance of furan over the temperature range 1464–1632 K is shown in Fig. 10. Linear regression leads to a value for $k_{overall} = 10^{15.3 \pm 0.3} \exp[(-326 \pm 8)\ \text{kJ mol}^{-1}/RT]\ \text{s}^{-1}$. Since furan is a moderately large molecule and our pressures are *ca.* 20 atm, we assume that this value has been obtained at or very near the high-pressure limit. This plot also contains the previous literature results.[4,5]

Discussion

Thermochemical Considerations

The interpretation of the Arrhenius parameters for the disappearance of furan and the development of a reaction model for product formation in the pyrolysis of furan is assisted by a consideration of the thermochemistry of the furan system. In an investigation of pyrolysis of the related compound, 2,5-dimethylfuran, Grela *et al.*[4] suggested that CO scission of this molecule could form a biradical intermediate which could

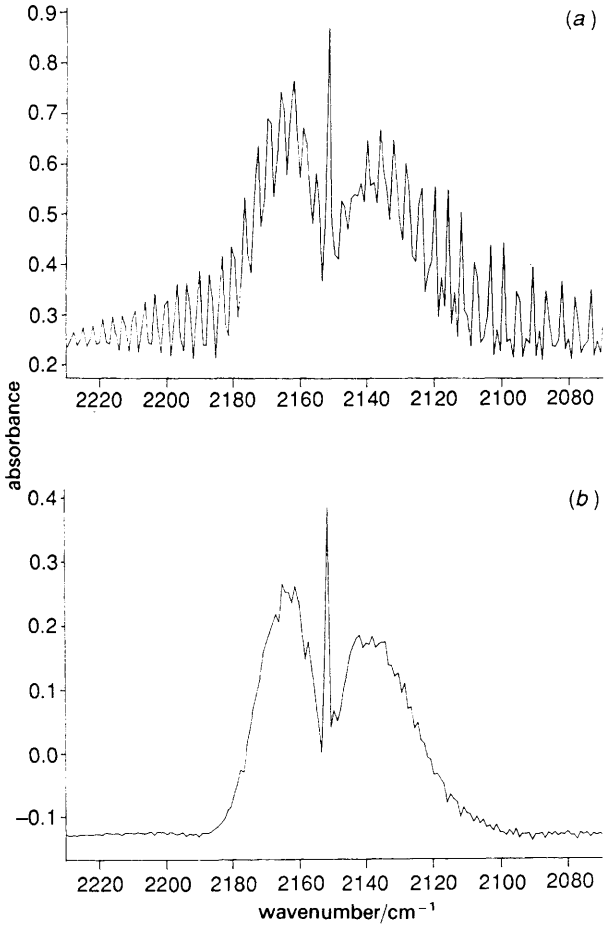

Fig. 8 (*a*) Typical FTIR spectrum of product gases showing overlapping peaks of CO and ketene; resolution 0.25 cm^{-1}; (*b*) FTIR spectrum of ketene with contribution from CO spectrum subtracted

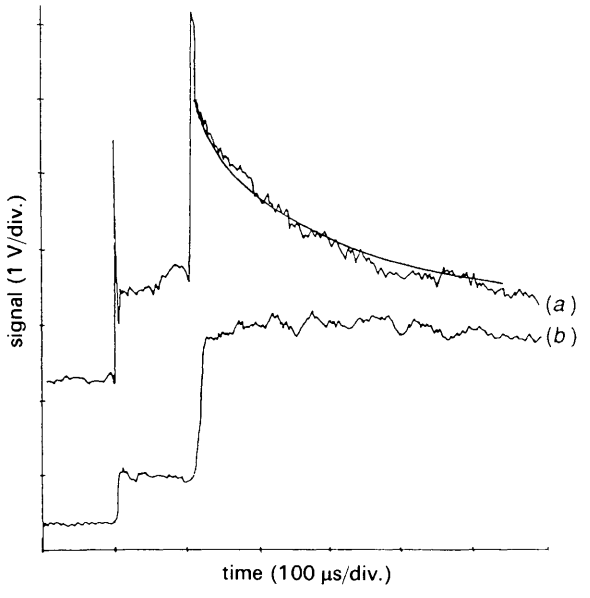

Fig. 9 Oscillograms of (*a*) variation in transmitted signal intensity from a CO_2 laser at 10.4 μm and (*b*) pressure trace measured at the same position for a reflected shock in a 2.0% furan mixture in Ar at 1584 K. The smooth decaying curve in (*a*) has been computed by fitting the integrated form of eqn. (v) to the experimental intensity data

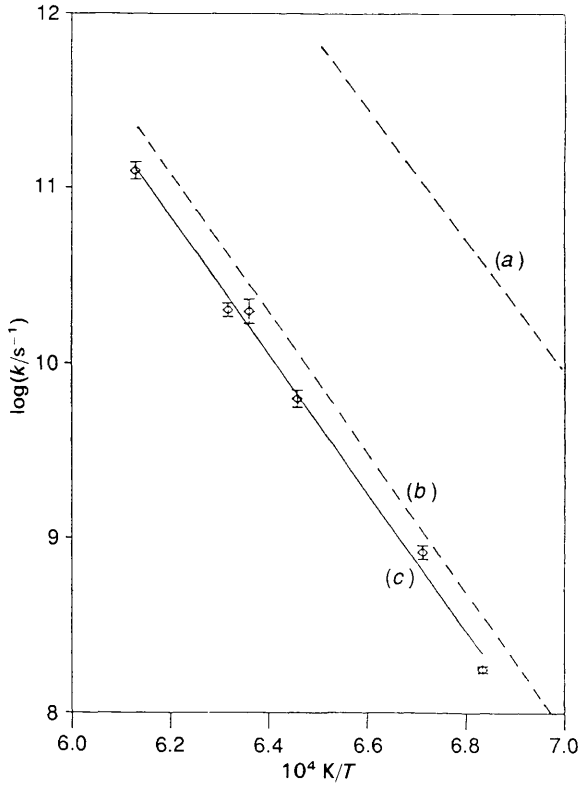

Fig. 10 Arrhenius plot of rate constants determined by laser absorption for furan decomposition. (*a*) extrapolated VLPP data[4]; (*b*) SPST data[5]; (*c*) present work

subsequently decompose to CO and C_5H_6 by one reaction channel, or to C_6H_6 and H_2O by a second channel.

Product distributions and stoichiometry suggest that the major overall processes in furan pyrolysis may be

$$C_4H_4O \rightleftharpoons C_3H_4 + CO; \qquad \Delta H^0_{r,300} = 109 \text{ kJ mol}^{-1} \quad (a)$$

$$C_4H_4O \rightleftharpoons CH_2CO + C_2H_2; \qquad \Delta H^0_{r,300} = 209 \text{ kJ mol}^{-1} \quad (b)$$

followed by secondary decomposition of propyne/allene and ketene. Indeed, Lifshitz *et al.*[5] suggested that reactions (*a*) and (*b*) were actually taking place. However, there are some problems associated with the adoption of reactions (*a*) and (*b*) for initiation of furan pyrolysis. First, in our work, acetylene and ketene were never found in equal concentrations. The excess of acetylene over ketene might be attributed to secondary reactions which produce acetylene (*e.g.*, the observed acceleration in C_2H_2 formation at temperatures above 1500 K when C_3H_4 concentrations started to decline) and/or the secondary decomposition of ketene. Secondly, the direct unimolecular elimination reaction of furan to propyne/allene and CO would require a hydrogen transfer from the C1 and C3 positions to C2 in the furan ring. It is difficult to postulate an activated complex for this reaction and the pre-exponential factor of such a reaction would be expected to be low (10^{12}–$10^{13.5}$ s^{-1}) since the reaction would involve a considerable decrease in the entropy of activation. The observed pre-exponential factor of $10^{15.3}$ s^{-1} and activation energy of 326 kJ mol^{-1} are strongly suggestive of a bond-breaking reaction.

The C—H bond dissociation energies for alkanes are *ca.* 389–410 kJ mol^{-1} whereas those of vinylic C—H range from 439 to 460 kJ mol^{-1} (ref. 12). We would expect the C—H bond dissociation energy to lie between that of alkanes and the vinyl group. Furan possesses considerable aromatic character[13] hence its C—C bond dissociation energy should

be similar to that in propene, *i.e. ca.* 423 kJ mol^{-1}. The observed activation energy for furan disappearance is thus considerably lower than that of any reasonable estimate for either C—H or C—C bond fission.

In contrast, C—O bond energies in ethers can be quite low, *e.g.*, the CH_3—OC_6H_5 bond energy[14] in methoxybenzene is only *ca.* 268 kJ mol^{-1}. However, on account of aromaticity, we would expect the C—O bond energy in furan to be higher than this value. We may estimate the C—O bond energy in furan by considering the thermochemistry of the biradical (I) formed by C—O bond scission.

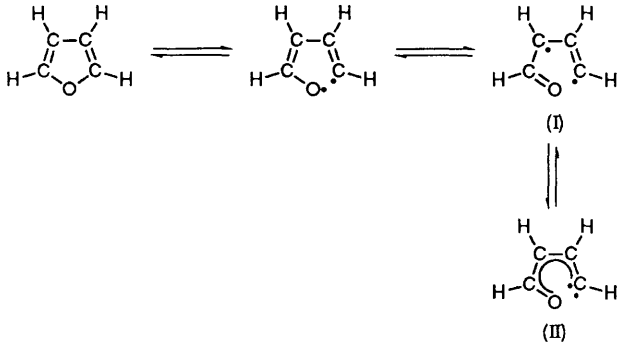

Using standard thermochemical group additivity techniques,[15] biradical (I) may be approximated by the following thermochemical groups:

$$CO—(C^{\bullet})(H) + C^{\bullet}—(CO)(C_d)(H) + C_d—(C^{\bullet})(H) + C_d^{\bullet}—(H)$$

where the terminology follows that of Benson.[15] Using the standard approximations[16] that $CO—(C^{\bullet})(H) \approx CO—(C)(H)$ and $C^{\bullet}—(CO)(C_d)(H) \approx C^{\bullet}—(CO)(C)(H)$, all groups are available in the thermochemical literature. Hence, $\Delta H^0_{f,300}(I) =$ 314 kJ mol^{-1}. The carbene form (II) should possess resonance stabilization compared with (I). We can estimate its enthalpy of formation by comparison with the analogous carbene formed in the isomerisation of allene to propyne. Honjou *et al.*[17] have made detailed *ab initio* computations of the C_3H_4 surface. They find that the carbene H—CH=CH—$\ddot{C}$H is more stable than the biradical H—$\dot{C}$H—CH=$\dot{C}$H and calculate $\Delta H^0_{f,300}$(H—CH=CH—$\ddot{C}$H) = 427 kJ mol^{-1}. By analogy, we can approximate (II) by the thermochemical groups

$$H—CH=CH—\ddot{C}H - C_d—(H)_2 + C_d—(C_d)(H) + CO—(C_d)(H).$$

Hence $\Delta H^0_{f,300}$(II) ≈ 427 − 26.2 + 28.4 − 132.6 = 297 kJ mol^{-1}.

Since $\Delta H^0_{f,300}(C_4H_4O) = -34.7$ kJ mol^{-1} (ref. 18), the C—O bond dissociation energy in furan and hence, the enthalpy of ring opening to a stabilized biradical, should be *ca.* 297 + 34.7 = 332 kJ mol^{-1}. This estimate is in good agreement both with our experimental activation energy for overall furan disappearance and with the value reported by Lifshitz *et al.*[5]

Reaction Model

It is postulated that furan decomposition is initiated by the unimolecular C—O ring scission to a biradical. It is further suggested that the biradical can undergo unimolecular decomposition *via* parallel reaction channels as shown in Fig. 11 and 12. The HCO radical will rapidly decompose into H + CO whilst the resonance-stabilized propynyl radical, C_3H_3, can undergo recombination to a precursor of benzene

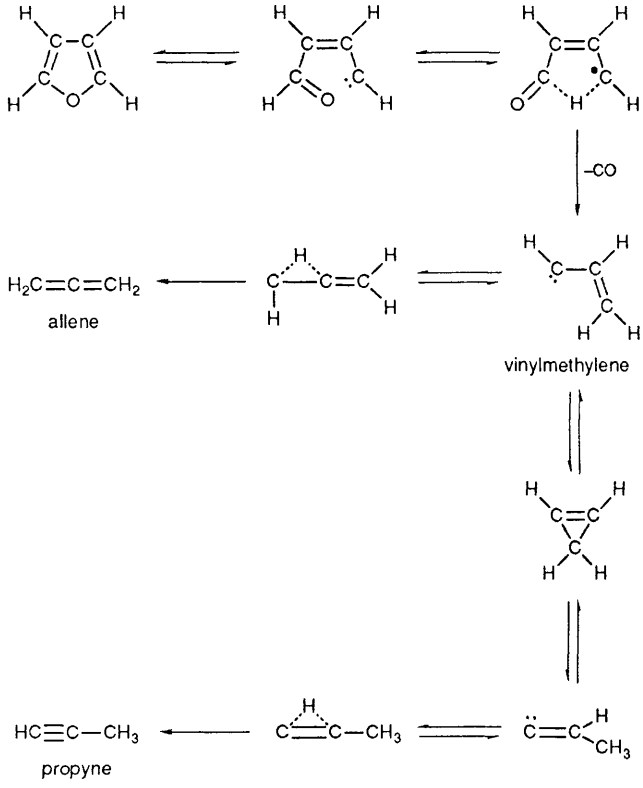

Fig. 11 Schematic diagram of the mechanism for the formation of propyne/allene

or abstract a hydrogen atom to form propyne. In all cases analogous rearrangements have already been identified on the C_3H_4 surface.[17] As shown in Fig. 11, elimination of CO from the biradical produces vinylmethylene which, as shown by Honjou *et al.*,[17] may either undergo a 1,2-H shift to allene

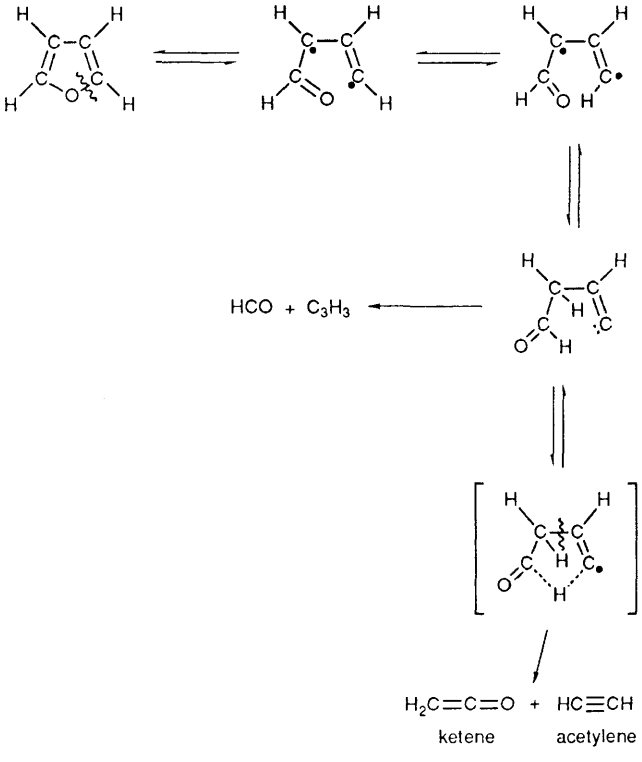

Fig. 12 Schematic diagram of the mechanism for the formation of acetylene and ketene

or rearrange *via* cyclopropene and propenylidene to propyne. Again, by analogy with C_3H_4 rearrangements,[17] the HCO + C_3H_3 and $CH_2CO + C_2H_2$ channels can take place *via* successive H atom shifts (Fig. 12).

A detailed reaction model has been developed to simulate the decomposition kinetics of furan and the formation of the products observed in the SPST experiments. The model is presented in Table 1. Rate constants for reverse reactions have been calculated from the forward rate constant and the equilibrium constant. Where not available in the thermochemical literature, thermodynamic quantities have been calculated by thermochemical group additivity techniques[15] and these values are given in Table 2.

As discussed previously, initiation by C—O ring scission is followed by the three-channel decomposition of the biradical denoted L-furan in Table 1 and which is identified with biradical (II). In the channel in which L-furan decomposes to allene/propyne and CO, rapid allene–propyne equilibration is attained *via* the vinylmethylene intermediate as shown by Honjou *et al.*[17] (see Fig. 11). This mechanism is described in the model by the reactions

$$\text{L-furan} \rightarrow C_3H_4(\text{propyne}) + CO; \qquad \Delta H^0_{r,300} = -209 \text{ kJ mol}^{-1} \quad (9)$$

$$\text{L-furan} \rightarrow C_3H_4(\text{allene}) + CO; \qquad \Delta H^0_{r,300} = -201 \text{ kJ mol}^{-1} \quad (10)$$

However, passage through the intermediate vinylmethylene is implicitly included through choice of the activation energies for reactions (9) and (10). Honjou *et al.*[17] have calculated the energies of the C_3H_4 activated complexes for propyne and allene. In the case of the activated complex for propyne they found it to be 280 kJ mol^{-1} above the ground state of

Table 1 Reaction model for furan pyrolysis[a]

	forward reaction			reverse reaction			
reactions[b]	log A	n	E	log A	n	E	ref.
1 furan → L-furan	15.34	0.0	326.4	11.22	0.0	4.2	PW
2 L-furan → HCO + C_3H_3	13.73	0.0	92.0	12.30	0.0	9.6	PW
3 H + furan → L-furyl + H_2	13.30	0.0	41.8	10.08	0.0	4.6	PW
4 L-furyl → CO + C_3H_3	12.00	0.0	41.8	10.43	0.0	50.2	PW
5 HCO + M → H + CO + M	14.32	0.0	61.5	14.47	0.0	0.4	23
6 HCO + H → H_2 + CO	14.08	0.0	0.0	14.84	0.0	375.7	24
7 C_3H_3 + H → propyne	12.70	0.0	0.0	15.27	0.0	373.2	est[c]
8 C_3H_3 + H → allene	12.70	0.0	0.0	14.43	0.0	364.4	est[c]
9 L-furan → CO + propyne	13.26	0.0	62.8	14.54	0.0	292.5	PW
10 L-furan → CO + allene	12.95	0.0	71.1	13.40	0.0	291.6	PW
11 L-furan → $CH_2CO + C_2H_2$	13.00	0.0	83.7	12.92	0.0	205.9	PW
12 H + HCCO → CH_2 + CO	14.04	0.0	0.0	13.86	0.0	133.1	25
13 CH_2CO → CH_2 + CO	15.56	0.0	246.9	13.28	0.0	−66.1	26[c]
14 $CH_2CO + CH_2 \rightarrow C_2H_4$ + CO	13.60	0.0	40.2	15.22	0.0	439.3	10
15 CH_2CO + H → CH_3 + CO	12.85	0.0	0.0	11.93	0.0	144.3	27
16 CH_2CO + H → HCCO + H_2	13.00	0.0	0.0	11.52	0.0	−9.2	est
17 H + propyne → $CH_3 + C_2H_2$	13.60	0.0	10.0	11.32	0.0	46.9	28
18 H + allene → $CH_3 + C_2H_2$	13.60	0.0	10.0	12.16	0.0	56.1	28
19 H + propyne → C_3H_3 + H_2	12.00	0.0	6.3	10.05	0.0	69.9	29
20 H + allene → C_3H_3 + H_2	12.00	0.0	6.3	10.88	0.0	79.1	29
21 CH_3 + propyne → $C_3H_3 + CH_4$	12.30	0.0	32.2	11.84	0.0	98.7	29
22 CH_3 + allene → $C_3H_3 + CH_4$	12.30	0.0	32.2	12.67	0.0	107.9	29
23 $CH_3 + H_2 \rightarrow CH_4$ + H	2.82	3.0	32.2	15.07	0.0	70.3	27
24 $2CH_3 \rightarrow C_2H_6$	12.85	0.0	0.0	16.17	0.0	365.7	30[c]
25 H + $C_2H_6 \rightarrow C_2H_5 + H_2$	2.74	3.5	21.8	14.54	0.0	88.7	27
26 $C_2H_5 \rightarrow C_2H_4$ + H	13.00	0.0	166.1	12.21	0.0	8.4	30[c]
27 H + $C_2H_2 \rightarrow C_2H_3$	12.64	0.0	10.0	12.37	0.0	179.1	31[c]
28 H + $C_2H_4 \rightarrow C_2H_3 + H_2$	13.70	0.0	33.5	11.84	0.0	27.6	10
29 2HCCO → C_2H_2 + 2CO	13.30	0.0	0.0	14.63	0.0	366.9	est
30 $CH_3 + C_3H_3 \rightarrow C_4H_6$	12.78	0.0	0.0	15.90	0.0	361.1	est[c]
31 $2C_3H_3 \rightarrow$ L-C_6H_6	12.70	0.0	0.0	15.05	0.0	244.8	est
32 $2C_3H_3 \rightarrow C_4H_4 + C_2H_2$	12.30	0.0	16.7	13.30	0.0	177.4	est
33 $2C_3H_3 \rightarrow C_2H_4 + C_4H_2$	12.30	0.0	16.7	13.86	0.0	176.6	est
34 C_3H_3 + HCCO → C_4H_4 + CO	13.30	0.0	0.0	15.19	0.0	340.6	est
35 HCCO + $CH_3 \rightarrow C_2H_4$ + CO	13.30	0.0	0.0	15.66	0.0	387.9	est
36 HCCO + C_2H_2 → CO + C_3H_3	13.00	0.0	8.4	13.89	0.0	188.7	est
37 $CH_2 + CH_3 \rightarrow C_2H_4$ + H	13.60	0.0	0.0	16.14	0.0	254.8	est
38 L-$C_6H_6 \rightarrow C_6H_6$	12.00	0.0	138.1	16.84	0.0	484.5	est
39 $C_2H_3 + C_3H_3 \rightarrow C_2H_2$ + propyne	13.00	0.0	0.0	15.84	0.0	204.6	est
40 $C_2H_3 + C_3H_3 \rightarrow C_2H_2$ + allene	13.00	0.0	0.0	15.01	0.0	195.4	est
41 C_2H_3 + propyne → $C_2H_4 + C_3H_3$	12.00	0.0	12.6	11.91	0.0	82.0	est
42 C_2H_3 + allene → $C_2H_4 + C_3H_3$	12.00	0.0	12.6	12.74	0.0	90.8	est
43 $C_2H_4 \rightarrow C_2H_2 + H_2$	12.97	0.0	323.0	11.38	0.0	148.5	32[c]
44 allene + $CH_2 \rightarrow C_2H_2 + C_2H_4$	13.00	0.0	0.0	14.10	0.0	300.8	est
45 $2C_2H_3 \rightarrow C_4H_6$	13.26	0.0	0.0	17.65	0.0	426.8	est[c]
46 $CH_3 + CH_2CO \rightarrow C_2H_5$ + CO	11.15	0.0	13.8	12.19	0.0	113.0	est

[a] Rate constants are of the form $k = AT^n \exp(-E/RT)$ where A, E are expressed in units of mol cm^3 s and kJ. PW indicates rate constant evaluated in the present work. est denotes rate constant estimated in the present work. [b] Species identification: L-furan, biradical (II) (see text); L-furyl, HC=CH—CH=C=O; C_4H_6, buta-1,3-diene; L-C_6H_6, hexa-1,5-diyne or one of the isomeric hexadienynes. [c] Pressure-dependent rate constant in fall-off region. Value is specific for the present pressure range.

Table 2 Thermochemical data for the furan system

species	$\Delta H^0_{f,300}$ /kJ mol^{-1}	S^0_{300} /J mol^{-1} K^{-1}	c_p^0/J mol^{-1} K^{-1}				
			300 K	500 K	1000 K	1500 K	2000 K
C_4H_4O[a]	−34.7	267.6	65.8	107.5	158.7	179.9	190.2
L-furan	276	332	94.5	118.8	155.5	172.7	180.9
L-furyl	216	298	91.9	117.4	145.6	157.4	166.5
L-C_6H_6[b]	414	341	108.7	156.7	217.2	243.0	248.2

[a] Data for furan is taken from ref. 18. [b] Calculated by group additivity for hexa-1,5-diyne.

propyne. Since these same transition states should exist for reactions (9) and (10), they should lie 63 and 71 kJ mol^{-1}, respectively, above L-furan. Thus, these two values have been adopted in the model for the activation energies of reactions (9) and (10). Values of A_9 and A_{10} have been obtained by fitting to the low-temperature propyne and allene concentration profiles. The minor channels from L-furan to C_2H_2 and ketene and to HCO and propynyl would be expected to have activation energies somewhat larger than those of reactions (9) and (10). Arrhenius parameters for these reactions, (11) and (2), respectively, have also been obtained by fitting.

The model also contains secondary reactions of the major products. These involve reactions with H atoms, generated initially from HCO decomposition but also at higher temperatures from decomposition of C_3H_4, and with methyl radicals. The relatively low concentrations of H_2 below 1500 K suggest that an H-chain decomposition of furan is not taking place.

Integration of the kinetic rate equations for the elementary reactions of Table 1 was made using the CHEMKIN package,[19] the stiff ordinary differential equation solver LSODE,[20] together with the SANDIA shock tube code[21] modified to allow for the effects of cooling by the reflected rarefaction wave in the shock tube. Rate of production and sensitivity analyses were carried out by means of the SENKIN program.[22]

Comparison of the kinetic model with experiment is given in Fig. 1–7. In Fig. 1 experimental values of the normalized concentration of furan remaining as a function of temperature are given for initial mixtures of 0.2, 1.0 and 2.0 mol.% of furan in argon. Experiment demonstrates clearly that the rate of disappearance of furan is first order in furan concentration. The model, computed for 0.2 and 2.0 mol.%, indicates that there is little dependence of the furan profiles on initial mixture composition. Agreement with experiment is good. The model also predicts the CO, C_3H_4, C_2H_2, CH_2CO, CH_4 and C_2H_4 profiles well up to 1600 K. Two minor products, vinylacetylene and benzene, are somewhat overpredicted by the model. The predicted C_4H_4 concentrations are a little high at 1500 K and continue to exceed observation at higher temperatures. This is not unexpected since the formation reactions of vinylacetylene have been described explicitly in the model whereas the high-temperature secondary decomposition reactions of this molecule have not specifically been included. Similarly, only the formation reactions of benzene have been modelled in detail and the model is therefore inadequate to predict the high-temperature secondary decomposition of C_6H_6. These decompositions take place only at temperatures where furan is more than 90% decomposed.

It should be pointed out that the pre-exponential factor for the initiation reaction (1) was increased from a value of $10^{15.3}$, obtained experimentally from the time-resolved IR spectra, to $10^{15.34}$ s^{-1} in the modelling. This is because the furan and product profiles are very sensitive to the rate constant of reaction (1) and optimization led to the latter value, just 10% larger than the experimental value. As may be seen from rate of production analysis, neglect in the experimental analysis of the reverse of reaction (1) leads to the lower value of A_1.

Rate of Production and Sensitivity Analyses

Detailed reaction flux calculations have been carried out using the reaction model to identify the important reaction pathways. The L-furan biradical plays a pivotal role in the decomposition mechanism and the relative flux through its various reaction channels is shown schematically in Fig. 13. The hydrogen abstraction reaction (3) is only a minor route for decomposition of furan. [Less than 1% of the reacting furan flux at 300 μs and 1450 K passes through reaction (3).] Flux calculations reveal that whilst ketene is principally produced *via* reaction (11) reaction (11) is only a minor route to acetylene. Most C_2H_2 is produced from H attack on C_3H_4 [reactions (17) and (18)]. This explains the experimental observation that $[C_2H_2]/[CH_2CO] > 1$.

Sensitivity analysis is useful in identifying the rate-determining steps in a detailed reaction model and in determining the effects that variation of the rate constant of a given reaction will have on reactant and products. Sensitivity analysis reveals that for each molecule, reaction (1), C—O fission, is strongly rate determining. Hence reaction (1) 'drives' the decomposition and is responsible for the

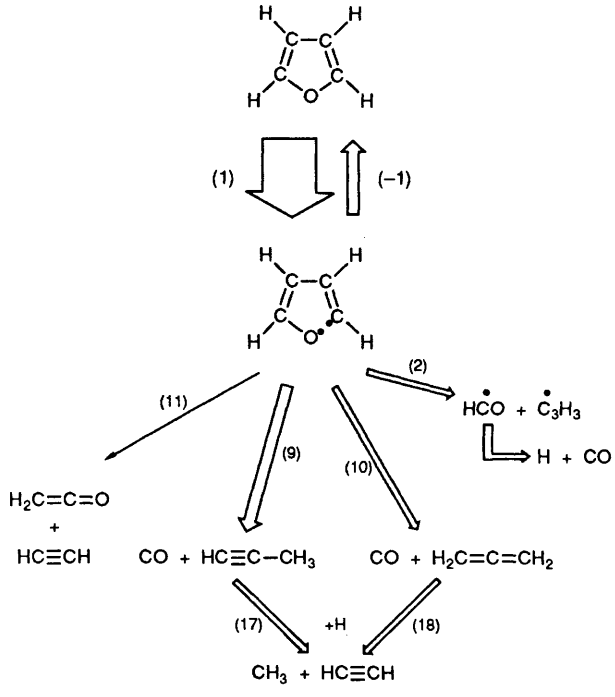

Fig. 13 The relative contribution of the principal reaction channels in the pyrolysis of furan. The thickness of the arrows indicates the relative fluxes

observed overall first-order kinetics and the first-order kinetics of formation of most of the products.

Conclusions

The thermal decomposition of furan diluted in argon exhibits overall kinetics first order in furan concentration. The rate constant for overall disappearance of furan has been measured over the temperature range 1464–1632 K at *ca.* 20 atm pressure by time-resolved IR spectroscopy and found to be $k_{overall} = 10^{15.3 \pm 0.3}$ exp[(-326 ± 8) kJ mol^{-1}/RT] s^{-1}. Thermochemical consideration and modelling studies are in agreement with the postulate of initiation by C—O ring scission to a biradical which can undergo further decomposition to propyne/allene and CO, acetylene and ketene and HCO and C_3H_3 radicals. Because of neglect in the experimental analysis of the small contribution of the reverse reaction, recyclization of the biradical, the pre-exponential factor of $A_1 = 10^{15.34}$ s^{-1} derived from the modelling studies, is likely to be the more accurate value. The Arrhenius parameters for overall disappearance of furan are in excellent agreement with the values reported previously by Lifshitz *et al.*[5]

The financial assistance of the Australian Research Council and of the Sir Zelman Cowen Universities Fund is gratefully acknowledged. Drs P. Browne and C. Little assisted with construction of the waveguide CO_2 laser. Mr. M. Esler is thanked for research assistance.

References

1 J. H. Lee and I. N. Tang, *J. Chem. Phys.*, 1982, **77**, 4459.
2 G. Holzer, J. Oro and W. Bertsch, *J. Chromatogr.*, 1976, **126**, 771.
3 J. Haggin, *Chem. Eng. News*, 1982, **60**, 17.
4 M. A. Grela, V. T. Amorebieta and A. J. Colussi, *J. Phys. Chem.*, 1985, **89**, 38.
5 A. Lifshitz, M. Bidani and S. Bidani, *J. Phys. Chem.*, 1986, **90**, 5373.
6 K. R. Doolan and J. C. Mackie, *Combust. Flame*, 1983, **50**, 29.
7 R. Gerlach and N. M. Amer, *Rev. Sci. Instrum.*, 1979, **50**, 1539.
8 E. Torneng, C. J. Nielsen, C. J. Klaeboe, H. Hope and H. Priebe, *Spectrochim. Acta*, 1980, **36**, 975.
9 J. B. Armitage, E. R. H. Jones and M. C. Whitting, *J. Chem. Soc.*, 1951, **55**, 44.
10 K. R. Doolan, J. C. Mackie and C. R. Reid, *Int. J. Chem. Kinet.*, 1986, **18**, 575.
11 J. N. Bradley, *Shock Waves in Chemistry and Physics*, Methuen, London, 1962.
12 D. F. McMillen and D. M. Golden, *Ann. Rev. Phys. Chem.*, 1982, **33**, 493.
13 R. M. Acheson, *An Introduction to the Chemistry of Heterocyclic Compounds*, Wiley, New York, 1976.
14 J. C. Mackie, K. R. Doolan and P. F. Nelson, *J. Phys. Chem.*, 1989, **93**, 664.
15 S. W. Benson, *Thermochemical Kinetics*, Wiley, New York, 2nd edn., 1976.
16 H. E. O'Neal and S. W. Benson, *Int. J. Chem. Kinet.*, 1969, **1**, 221.
17 N. Honjou, J. Pacansky and M. Yoshimine, *J. Am. Chem. Soc.*, 1985, **107**, 5332.
18 G. B. Guthrie, D. W. Scott, W. N. Hubbard, C. Katz, J. P. McCullough, M. E. Gross, K. D. Williamson and G. Waddington, *J. Am. Chem. Soc.*, 1952, **74**, 4662.
19 R. J. Kee, J. A. Miller and T. H. Jefferson, CHEMKIN: A General-Purpose Problem-Independent Chemical Kinetics Code Package, SANDIA Report SAND80-8003, Sandia National Laboratories, Albuquerque, NM, 1980.
20 A. C. Hindmarsh, LSODE and LSODI: Two New Initial Value Differential Equation Solvers, ACM Signum Newsletter, 1980, **15**, 4.
21 R. E. Mitchell and R. J. Kee, A General-Purpose Computer Code for Predicting Chemical Kinetic Behavior behind Incident and Reflected Shocks, SANDIA Report SAND82-8205, Sandia National Laboratories, Albuquerque, NM, 1982.
22 A. E. Lutz, R. J. Kee and J. A. Miller, SENKIN: A Fortran Program Predicting Homogeneous Gas Phase Chemical Kinetics with Sensitivity Analysis, SANDIA Report SAND87-8248, Sandia National Laboratories, Albuquerque, NM, 1988.
23 A. M. Dean, B. L. Craig, R. L. Johnson, M. C. Schultz and E. E. Wang, *17th Symp. (Int.) on Combustion*, The Combustion Institute, Pittsburgh, 1979, p. 577.
24 V. A. Nadtochenko, O. M. Sarkisov and V. I. Vedeneev, *Dokl. Akad. Nauk SSSR*, 1979, **224**, 152.
25 P. Glarborg, R. J. Kee and J. A. Miller, *Combust. Flame*, 1986, **65**, 177.
26 H. Gg. Wagner and F. Zabel, *Ber. Bunsenges. Phys. Chem.*, 1971, **75**, 114.
27 J. Warnatz, *Rate Coefficients in the C/H/O System, in Combustion Chemistry*, ed. W. C. Gardiner, Springer-Verlag, New York, 1984, ch. 5.
28 C. H. Wu and R. D. Kern, *J. Phys. Chem.*, 1987, **91**, 6291.
29 J. H. Kiefer, M. Z. Al-Alami and K. A. Budach, *J. Phys. Chem.*, 1982, **86**, 808.
30 D. L. Baulch and J. Duxbury, *Combust. Flame*, 1980, **37**, 313.
31 W. A. Payne and L. J. Stief, *J. Chem. Phys.*, 1976, **64**, 1150.
32 T. Just, P. Roth and R. Damm, *16th Symp. (Int.) on Combustion*, The Combustion Institute, Pittsburgh, 1977, p. 961.

Paper 0/03980B; *Received* 3rd *September*, 1990